

Palladium nanoparticles/wool keratin-assisted carbon composite-modified flexible and disposable electrochemical solid-state pH sensor

Wenli Zhang(张文立), Xiaotian Liu(刘笑天), Youhui Lin(林友辉), Liyun Ma(马利芸), Linqin Kong(孔令庆), Guangzong Min(闵光宗), Ronghui Wu(吴荣辉), Sharwari K. Mengane, Likun Yang(杨丽坤), Aniruddha B. Patil, and Xiang Yang Liu(刘向阳)

Citation: Chin. Phys. B, 2022, 31 (**2**): 028201. DOI: 10.1088/1674-1056/ac3ca9

Journal homepage: http://cpb.iphy.ac.cn; http://iopscience.iop.org/cpb

What follows is a list of articles you may be interested in

Optical strong coupling in hybrid metal-graphene metamaterial for terahertz sensing

Ling Xu(徐玲), Yun Shen(沈云), Liangliang Gu(顾亮亮), Yin Li(李寅), Xiaohua Deng(邓晓华), Zhifu Wei(魏之傅), Jianwei Xu(徐建伟), and Juncheng Cao(曹俊诚)

Chin. Phys. B, 2021, 30 (**11**): 118702. DOI: 10.1088/1674-1056/abfb58

Detection of HIV-1 antigen based on magnetic tunnel junction sensors

Li Li(李丽), Kai-Yu Mak(麦启宇), Yan Zhou(周艳)

Chin. Phys. B, 2020, 29 (**8**): 088701. DOI: 10.1088/1674-1056/ab928d

Effects of rapid thermal annealing on room temperature NO_2-sensing properties of WO_3 thin film under LED radiation

Hu Ming, Jia Ding-Li, Liu Qing-Lin, Li Ming-Da, Sun Peng

Chin. Phys. B, 2013, 22 (**6**): 068204. DOI: 10.1088/1674-1056/22/6/068204

The light-enhanced NO_2 sensing properties of porous silicon gas sensors at room temperature

Chen Hui-Qing,Hu Ming,Zeng Jing,Wang Wei-Dan

Chin. Phys. B, 2012, 21 (**5**): 058201. DOI: 10.1088/1674-1056/21/5/058201

Palladium nanoparticles/wool keratin-assisted carbon composite-modified flexible and disposable electrochemical solid-state pH sensor

Wenli Zhang(张文立)[1], Xiaotian Liu(刘笑天)[1], Youhui Lin(林友辉)[1], Liyun Ma(马利芸)[1], Linqing Kong(孔令庆)[1], Guangzong Min(闵光宗)[1], Ronghui Wu(吴荣辉)[1], Sharwari K. Mengane[2], Likun Yang(杨丽坤)[1,†], Aniruddha B. Patil[3,‡], and Xiang Yang Liu(刘向阳)[1,§]

[1] *Department of Physics, College of Materials, and Shenzhen Research Institute of Xiamen University, Xiamen University, Xiamen* 361005, *China*
[2] *Department of Botany, M.H. Shinde Mahavidyalaya, Tisangi, Kolhapur* 416226, *India*
[3] *Department of Chemistry, M. D. College, Parel, Mumbai*-400012, *India*

(Received 29 July 2021; revised manuscript received 16 November 2021; accepted manuscript online 24 November 2021)

Several pH-dependent processes and reactions take place in the human body; hence, the pH of body fluids is the best indicator of disturbed health conditions. However, accurate and real-time diagnosis of the pH of body fluids is complicated because of limited commercially available pH sensors. Hence, we aimed to prepare a flexible, transparent, disposable, user-friendly, and economic strip-based solid-state pH sensor using palladium nanoparticles (PdNPs)/N-doped carbon (NC) composite material. The PdNPs/NC composite material was synthesized using wool keratin (WK) as a precursor. The *in-situ* prepared PdNPs played a key role in the controlled switching of protein structure to the N-doped carbon skeleton with π–π arrangement at the mesoscale level, which mimics the A–B type polymeric structure, and hence, is highly susceptible to H^+ ions. The optimized carbonization condition in the presence of PdNPs showed that the material obtained using a modified Ag/AgCl reference electrode had the highest pH sensitivity with excellent stability and durability. The optimized pH sensor showed high specificity and selectivity with a sensitivity of 55 mV/pH unit and a relative standard deviation of 0.79%. This study is the first to synthesize PdNPs using WK as a stabilizing and reducing agent. The applicability of the sensor was investigated for biological samples, namely, saliva and gastric juices. The proposed protocol and material have implications in solid-state chemistry, where biological material will be the best choice for the synthesis of materials with anticipated performance.

Keywords: palladium nanoparticle, electrochemical sensor, solid-state pH sensor, flexible strip sensor

PACS: 82.47.Rs, 87.85.fk **DOI:** 10.1088/1674-1056/ac3ca9

1. Introduction

Accurate and early diagnosis of any disease plays a crucial role in the quick and complete recovery of patients. In the human body, several pH-dependent processes and reactions take place; hence, the pH of body fluids is the best indicator of the disturbed health condition.[1] For example, frequent checking of the pH level of sweat from the skin helps understand the pathogenesis of skin diseases, including atopic dermatitis and acne vulgaris.[2–4] The alkaline pH value in the range of 7 to 8.5 of wound skin indicates the deterioration of the wound, which helps medical surgeons to decide or change medication regimen.[5] However, accurate and real-time diagnosis of the pH of body fluids is complicated because of limited commercially available pH sensors.

The quantity of biological samples, especially sweat, saliva, serum, and tears, is considerably low, and therefore, conventional pH sensors such as glass electrodes are inoperable in the case of biological fluids. Hence, an electrochemical solid-state strip-based pH sensor would be the best choice.[6] Electrochemical pH sensors work on the principle of deprotonation of H^+ ions present on the surface of working electrode material in the presence of reference electrode Ag/AgCl.[7] The deprotonation of H^+ ions is recorded as a change in open circuit potential value, which is equivalent to the concentration of H^+ ions.

Materials having the long-chain conjugated π–π system with heteroatom exhibit high affinity toward H^+ ions; hence, A–B type polymeric materials would be the best choice.[8] Recently, several materials such as polyaniline (PANI), polypyrrole modified PANI, graphene, AuNPs/activated carbon, and metal oxides have been used in pH sensors.[2,4,7,9] Although PANI is exclusive because of the A–B type conjugated structure, it losses conductivity in solutions of pH $>$ 7; hence, PANI is not suitable for high pH solutions and long-term usage.[3]

This study aimed to prepare a strip-based solid-state pH sensor using PdNPs/NC composite material. We successfully prepared PdNPs for the first time using wool keratin (WK) as a stabilizing and reducing agent. The PdNPs/NC-500-modified sensor exhibited the highest pH sensitivity with excellent sta-

†Corresponding author. E-mail: lkyang@xmu.edu.cn
‡Corresponding author. E-mail: aniruddhapatil135@gmail.com
§Corresponding author. E-mail: liuxy@xum.edu.cn

© 2022 Chinese Physical Society and IOP Publishing Ltd

bility and durability. Therefore, the study findings have strong implications in solid-state chemistry as the developed sensor can be used for biological samples, including saliva and gastric juices.

2. Materials and methods

2.1. Chemical reagents and apparatus

Wool fibers (WF) (Merino 64's) were purchased from Tongxiang Dushi Woolen Material Co., Ltd. Palladium chloride ($PdCl_2$) was purchased from Sigma Aldrich; sodium bicarbonate and ethyl alcohol with the purity of $> 99.5\%$ were purchased from Sinopharm Chemical Reagent. Citric acid monohydrate, sodium dodecyl sulfate, urea, sodium hydroxide, disodium hydrogen phosphate dodecahydrate, sodium chloride, and sodium sulfide nonahydrate with the purity of > 99 were purchased from Xilong Chemical Industry. Poly (vinyl butyral) (PVB) (M.W. 90000–120000) was obtained from Shanghai Macklin Biochemical Co. Ltd. 5% Nafion PFSA polymer (Dispersion D520) was obtained from OU Point Ltd. The water used in all experiments was ultra pure (the resistivity > 18 MΩ·cm^{-1}). Except for wool, all chemicals were used without any purification process.

2.2. Preparation of regenerated WK solution

The standard reduction protocol was followed for the extraction of WK from raw WF.[12] Thereafter, 12.5 g of WF was added in a 250-mL aqueous solution of urea, Na_2S, and SDS. The concentration of urea, Na_2S, and SDS was 4 M, 0.1 M, and 0.02 M, respectively. The reaction mixture was then stirred at 45 °C for 12 h and then filtered and dialyzed against ultra-pure water (18 MΩ) using a dialysis bag (Solarbio, molecular cut-off about 3500 Da) for 3 days with frequent change of water. Next, the extracted WK was concentrated to 5 wt% by heating at 60 °C for 8 h and was then stored at 4 °C.

2.3. Preparation of PdNPs/WK

In 5 mL of 10 mM aqueous solution of $PdCl_2$, 5 mL of WK solution was added with vigorous stirring. Next, 1 M NaOH solution was added slowly to adjust the pH of the reaction mixture between 10 and 12. The reaction mixture was retained for 6 h at 90 °C till the pale yellow color of the suspension turned dark brown.

2.4. Preparation of PdNPs/WK composite sponges

The reaction mixture was freeze-dried and transformed into a spongy form. In the actual production process, the PdNPs/WK water suspension (without dialysis) was stored in the mold, frozen at −20 °C for one day until the suspension was completely frozen, and then placed in a freeze dryer, the temperature was set at −106 °C, and freeze-dried in vacuum for two days. The water was completely removed to obtain a three-dimensional (3D) porous composite sponge.

2.5. Preparation of PdNPs/NC

The pyrolysis of the obtained solid mass was performed stepwise to obtain the anticipated structure. Temperature programming is the key factor in controlling the emission of volatile gases. In a tube furnace under nitrogen atmosphere, the solid mass of PdNPs/WK was heated at 150 °C for 60 min, then heated up to 350 °C (2 °C·min^{-1}) for 60 min, and finally up to 700 °C at a rate of 2 °C·min^{-1} to get the polyaromatic N-doped porous carbon structure. The PdNPs/NC were washed multiple times with deionized water to clarify salt residual content and dried overnight at 60 °C.

2.6. Characterization of PdNPs/NC

An x-ray diffractometer (XRD, Bruker D8 AVANCE) was used for the crystallographic phase identification. The surface morphology, position of PdNPs in the composite materials, and lattices of PdNPs were analyzed by transmission electron microscopy (TEM) using JEM-2100F (JEOL, Japan). Raman spectra were obtained using (HORIBA Lab RAM HR Evolution) with a 532-nm excitation laser. The efficiency of the fabricated pH sensor was confirmed and compared with the commercial pH meter (Thermo Scientific).

2.7. Fabrication of the flexible strip sensor

The two-electrode electrochemical sensor consisting of a working electrode and a reference electrode was prepared. Figure 3 shows the complete protocol of the fabrication process of the two-electrode pH sensor, in which the mask pattern was initially designed and cut by laser-cutting technology and attached to the polyethylene terephthalate film. The desired conductive pattern was obtained by the magnetron sputtering technique. Finally, the paper mask was peeled off to obtain a flexible sensor substrate with double electrode patterning. The two electrodes were designed in parallel, and the insulation between the two electrodes of the sensor was ensured.

2.7.1. Preparation of ink for the pH-sensing working electrode material

A series of pH-sensing working electrode inks were prepared using carbonized composite materials, namely, PdNPs/NC-400, PdNPs/NC-500, PdNPs/NC-600, and PdNPs/NC-700. Briefly, 5 mg of accurately weighted carbonized composite material was dispersed in 1 mL of the aqueous solution containing 10% Nafion binder. The solution was subjected to ultrasound treatment for 10 min to acquire a uniformly dispersed solution.

PVB solution was obtained by melting PVB into methanol at a concentration of 76 mg/mL. Fine KCl powder with a diameter of about 50–200 μm was obtained from KCl particles using ball milling for 0.5 h. A total of 3.5 g of KCl powder was mixed with 3 mL of PVB solution to form

PVB/KCl suspension. The solution was subjected to ultrasound treatment for 10 min to get a uniformly dispersed solution of PVB above KCl solution.

2.7.2. Development of working electrode and reference electrode

The working electrode was prepared by the drop-casting technique, in which 10 μL of water-based suspension was cast in the working area and dried for 10 min in a vacuum at 60 °C.

The reference electrode was prepared by screen printing of the Ag/AgCl layer and a polymer layer. Here, 3 μL of silver nanowires solution was dropped on the reference electrode area and allowed to dry in an oven for about 2 min. Thereafter, 10 μL of $FeCl_3$ solution (concentration of 0.05 m/L) was added and allowed to chlorinate Ag for 5 s. After chlorination, $FeCl_3$ was removed by quick immersion of the sensor in pure water to obtain the Ag/AgCl layer. Next, the layer of PVB/KCl suspension on the reference electrode was prepared by the screen printing method, and the sensor was transferred to an oven (60 °C) for drying for 10 min.

3. Results and discussion

Figure 1 presents the scheme for the *in-situ* synthesis of PdNPs-doped mesoporous carbon composites using WK. A total of 5 mL of 10 mM $PdCl_2$ aqueous solution was added in 5 mL of WK solution (2.5 wt%), and the reaction mixture was adjusted to the pH of 1–12 under strong agitation. The solution was stored at 75 °C for 12 h to form a complex solution of PdNPs and WK (PdNPs/WK). At the molecular level, WK has some remarkable structural aspects, which can be manipulated to get the desired performance. The first aspect is WK molecules composed of up to 40% proteins (amino acids) that can be transferred to N-doped aromatic carbon by heat treatment.[12] The second aspect is WK disulfide crosslinkage, which is extremely beneficial for stabilizing the structure of wool fibers.[13,14] Some disulfide bonds break during the formation of the WK solution. Each broken disulfide bond is divided into two sulfhydryl groups (–SH), which are unstable and active and can be used as a reducing agent.[15] These unstable sulfhydryl groups can reduce Pd ions to atomic Pd and are embedded or adsorbed on the lamellar space or the surface of regenerated WK through strong interactions with amino groups[19] and are firmly fixed in the unique precursor framework (Fig. 1). The prepared PdNPs/WK composite mixtures were converted to spongy solid masses using the freeze-drying technique. The prepared solid mass was carbonized in a nitrogen atmosphere at different carbonization temperatures (400–700 °C) to obtain the ordered porous carbon structure. The obtained PdNPs-doped carbon composites were named as PdNPs/NC-400, PdNPs/NC-500, PdNPs/NC-600, and PdNPs/NC-700.

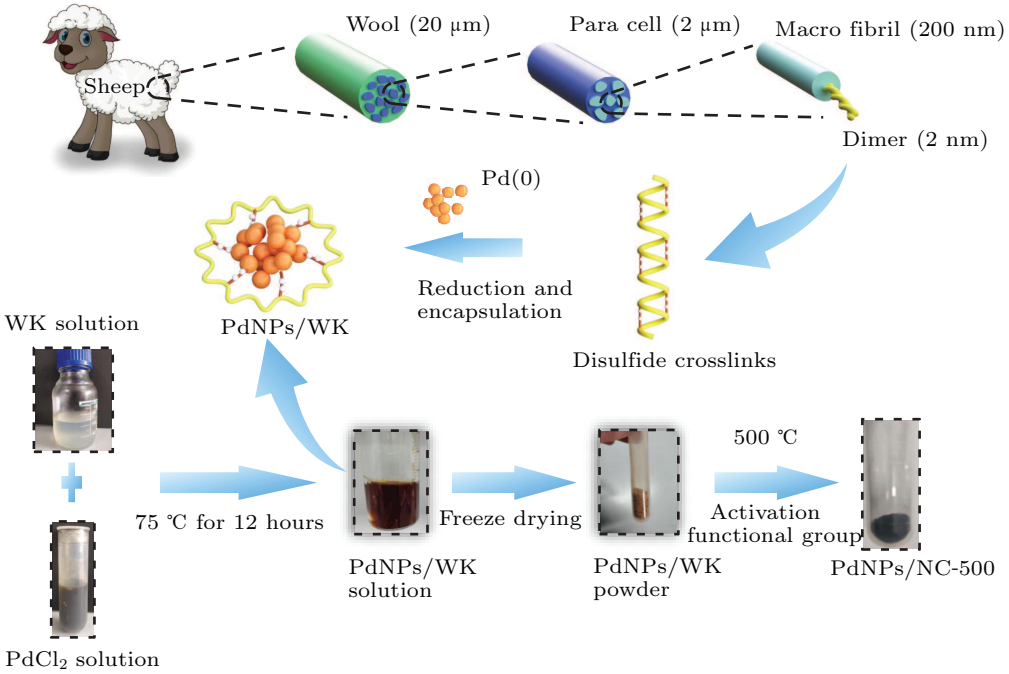


Fig. 1. Schematic illustration of the molecular structure of wool keratin as a multifunctional biological protein material for *in-situ* preparation and engineering of PdNPs/NC composite materials and synthesis of PdNPs/NC using the controlled preparation protocol.

3.1. Modification of microstructure

In pyrolysis, the surface morphology of materials depends on the percentage emission of the volatile matter.[16] Nobel metal nanoparticles play a catalytic role in the emission of such volatile components. Here, the *in-situ* prepared PdNPs of the composite mass catalyzed and accelerated the emission of carbon and nitrogen oxides; thus, resulting in the highly

porous and aromatized carbon structure.[11]

The surface morphology of PdNPs was investigated by high-resolution TEM (HR-TEM) analysis. Figures 2(a) and 2(b) present the HR-TEM images of the PdNPs/WK composite mass, showing well-dispersed PdNPs in the spongy WK. Figure 2(c) presents the HR-TEM image, showing well-dispersed PdNPs with the lattice pattern of PdNPs (0.21 nm). Figure 2(d) presents energy dispersive spectroscopy analysis that confirms the presence of PdNPs. Figures 2(e)–2(h) shows mapping analysis results, indicating the presence of nitrogen and PdNPs in the composite material. The XRD images confirmed the crystallinity of the composite (Fig. 2(i)). The diffraction peak of the PdNPs/NC composite at $2\theta = 40$ represents the graphite plane (110), whereas three strong diffraction peaks at (200) and (220) indicate the presence of PdNPs. The diffraction peaks of the synthesized PdNPs are located at the same angle as the diffraction patterns of bulk Pd from the Joint Committee on Powder Diffraction Standards (JCPDS: 65–2870), confirming the formation of Pd nanoparticles in the composite. Raman spectra of the composite PdNPs/NC confirmed the domain structure and structural assembly of the synthesized composite (Fig. 2(j)). All spectra showed two significant bands: the D-band is usually attributed to the disordered surface morphology, and the G-band is attributed to C–C symmetric stretching. We observed two bands, at 1363 cm^{-1} and 1601 cm^{-1}, which were used to characterize the Raman spectra and can be attributed to the D and G bands of PdNPs/NC nanocomposites. The obtained results showed two remarkable observations: first, with the increasing temperature, the strength of the G-band increases, showing increased sp^2 carbon content. Second, from 400 °C to 700 °C, with the increase in temperature, the I_D/I_G ratio increases up to 1.02 and then decreases to 0.97. This result indicates that the surface area increased due to the emission of gases with increasing temperature, and at high temperature, the surface area decreased due to the sintering effect.

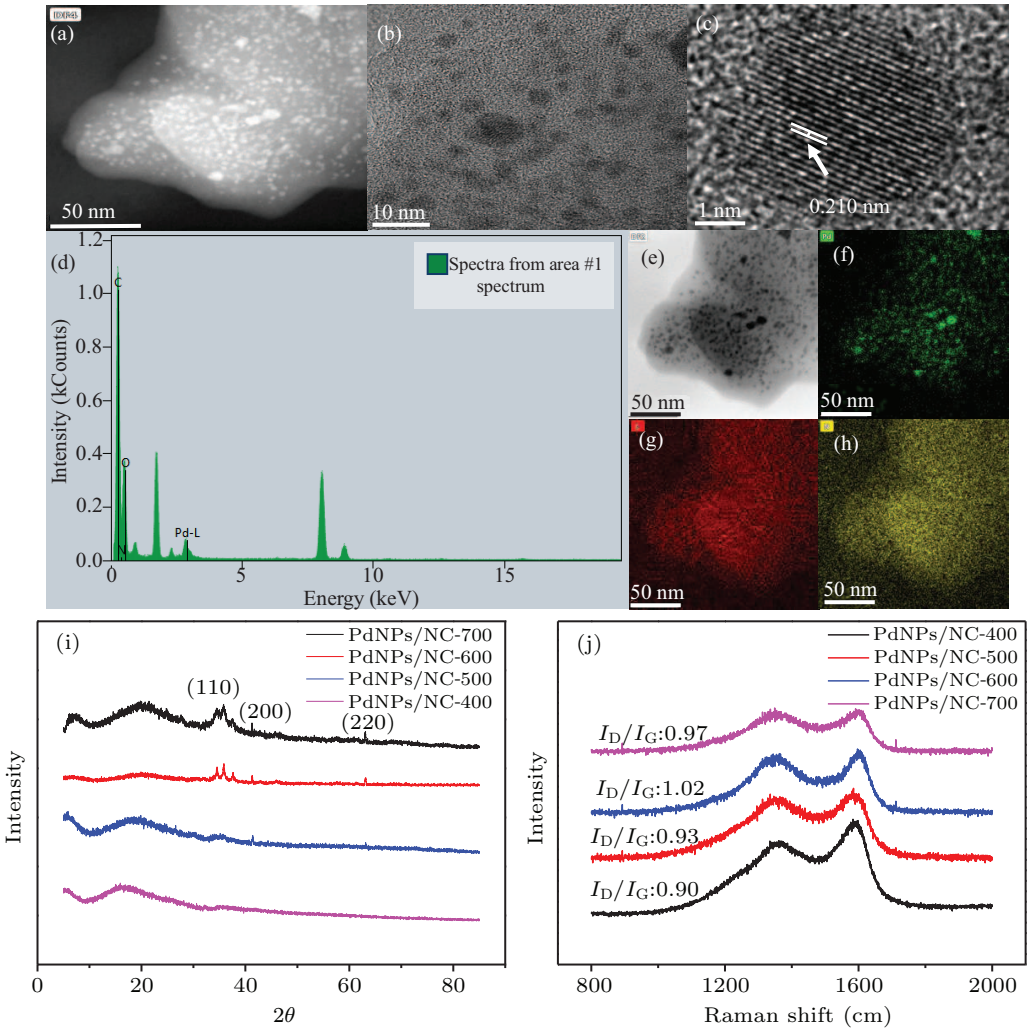


Fig. 2. Effect of the carbonization temperature on the carbon skeleton and morphology of PdNPs. (a)–(c) PdNPs/NC transmission electron microscopy (TEM) and high-resolution TEM image; (d) the energy dispersive spectroscopy diagram of PdNPs/NC; (e)–(h) element mapping; (i) corresponding x-ray diffraction pattern; (j) corresponding Raman spectra.

3.2. The A–B type composite pH sensor

The carbonized PdNPs/NC materials were used to fabricate the two-electrode flexible strip sensor for detecting the exact pH value of body fluids[20] (Fig. 3). A series of four different pH sensors were prepared by changing the working electrode ink materials, namely, PdNPs/NC-400, PdNPs/NC-500, PdNPs/NC-600, and PdNPs/NC-700.

In principle, the pyrolyzed nitrogen-containing carbon skeleton acts as the A–B type polymeric material, in which the aromatized carbon part signifies the A section and N dopant signifies the B section, and their combination reveals the unique π-type conjugate structure. The prepared composite mass functions as the A–B type solid-state pH-sensitive material such as functionalized PANI structure sensitive for H^+ ions. The presence of PdNPs in the vicinity of the material enhances the performance of the material due to its extraordinary affinity toward H^+ ions. We studied the results of a continuous cycle test of the sensor in phosphate buffer (pH: 3 to 9) (Fig. 4(a)). The PdNPs/NC-500-modified sensor demonstrated the highest sensitivity of 55 mV/pH with a relative standard deviation (RSD) of 0.79%.

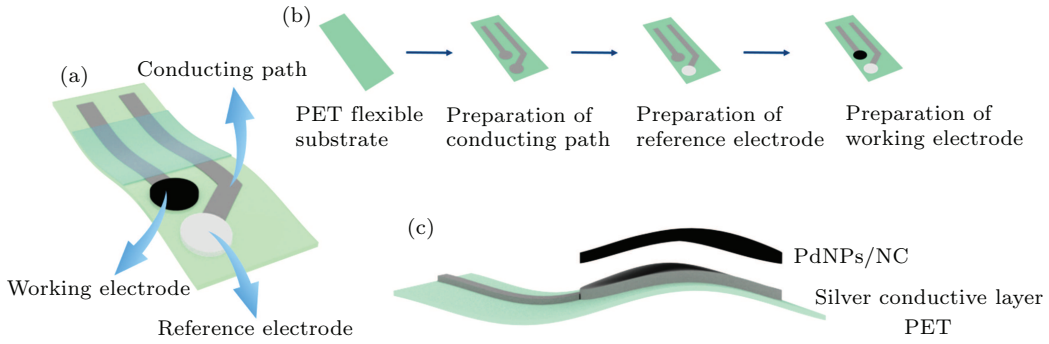


Fig. 3. The pH sensor. (a) Schematic illustration of two-electrode flexible strip-based sensor. (b) Fabrication process of the two-electrode pH sensor. (c) Schematic illustration of the vertical cross-section of the working electrode.

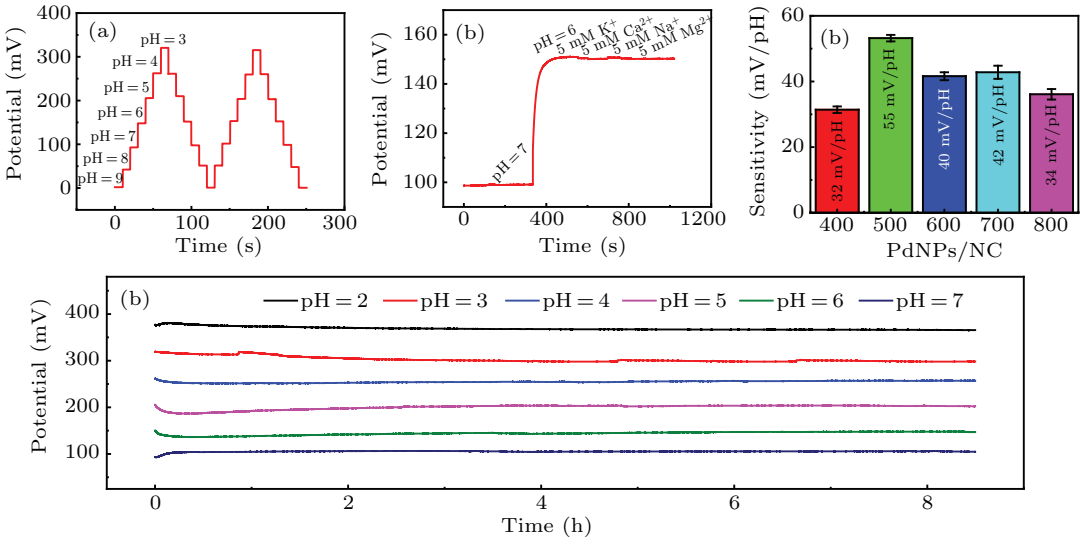


Fig. 4. General performance and response of pH sensor: (a) sensitivity and repeatability of the pH sensor in the pH range of 3–9; (b) selectivity (anti-interference) of PdNPs/NC-500 modified pH sensor; (c) pH sensitivity comparative results of the carbonized composites; (d) stability of the PdNPs/NC-500-modified pH sensor in different conditions.

The composite material-modified sensors were further tested and applied for biochemical applications, in which the sensitivity, selectivity, stability, reproducibility of the sensor were examined. As the pH of body fluids usually fluctuates between 3.5 and 8,[3] the response of the prepared PdNPs/NC-modified sensor was investigated at pH 3 to 9 (Fig. 4(a)). For the detection of a biological sample, the selectivity, sensitivity, and accuracy of the sensor are critical. Figure 4(b) presents the selectivity analysis of the PdNPs/NC-500 modified sensor toward H^+ ions; herein, the performance of the sensor was recorded for the solutions of 5 mM Ca^{2+}, 5 mM K^+, 5 mM Mg^{2+}, and 5 mM Na^+ at pH 6 and 7. No considerable change was observed in the potential values except for pH 6 and pH 7 buffer solutions, which indicates the selectivity of the sensor toward H^+ ions only. The sensitivity of all materials is shown in Fig. 4(c), in which the PdNPs/NC-500-modified sensor showed the highest sensitivity of 55 mV/pH. Figure 4(d) shows the stability of the PdNPs/NC-500-modified sensor, in which the sensor response was investigated for 9 h at pH 2, 3, 4, 5, 6, and 7. The obtained results showed excellent

stability response with only 2.9 mV (the average) deviation in the potential value even after 9 h consistent measurement; this singular performance of the sensor is attributed to the stringent surface morphology of PdNPs/NC-500.

Table 1. Comparison among different electrochemical sensors proposed for the determination of pH.

pH sensing material	Sensitivity (mV/pH)	RSD %	Ref.
Graphene oxide	40	0.15%	[17]
Poly (terthiophene benzoic acid)/AuZn alloy oxide	58.5 ± 0.87	2.0%	[18]
PANI/carbon fiber	50.1	3.72%	[2]
PANI/gold	62.5	1.0%	[7]
PdNPs/NC-500	55	0.79%	this work

The PdNPs/NC-500-modified pH sensor was tested repeatedly for eight consecutive cycles, in which the response of the sensor was examined for pH 2 to 7 buffer solutions (Fig. 5(a)). In both ascending and descending cycles from pH 2 to 7 and again to 2 with one-unit increments, the results revealed an average slope of 55 mV/decade with RSD 0.79%, which is better than other available solid-state pH sensors (Table 1). To explore the linearity and sensitivity between different pH sensors prepared in the same batch of materials, we used a batch of materials to prepare three samples to verify the linearity of pH-potential of each sensor under the same condition. The results are shown in Fig. 5(b). The linearity of this sensor is extremely high, $R^2 = 0.9976$. Sensitivity is one of the important criteria to determine whether the sensor is excellent or bad. Here, we measured the sensitivity using multiple sensors (Fig. 5(c)), in which the sensitivity of all sensors reached 55 ± 2 mV/pH. This is above the average sensitivity for most miniature pH sensors, thus highlighting the superiority of this sensor. To study the reproducibility of the material synthesis protocol, four parallel sensors were prepared using PdNPs/NC-500 working electrode materials from four different batches obtained by the same synthesis protocol. Figures 5(d) and 5(e) show the responses of all four group samples for buffer solutions from pH 2 to 7 and then from pH 7 to 2 with an increase of pH 1, in which the linear trend in responses of all four material samples with negligible variation in potential value was observed. Furthermore, the durability/stability of the sensor was investigated. The PdNPs/NC-500-modified sensor was stored at room temperature for a week and used for analysis. Figure 5(f) shows the daily response of the sensor, in which the average sensitivity of the sensor was calculated, which demonstrated extra-high stability and more than 98% similarity with the pH sensor performance even after one week. These results indicated that the prepared PdNPs/NC-500-modified pH sensors provide accurate and reliable analytical results.

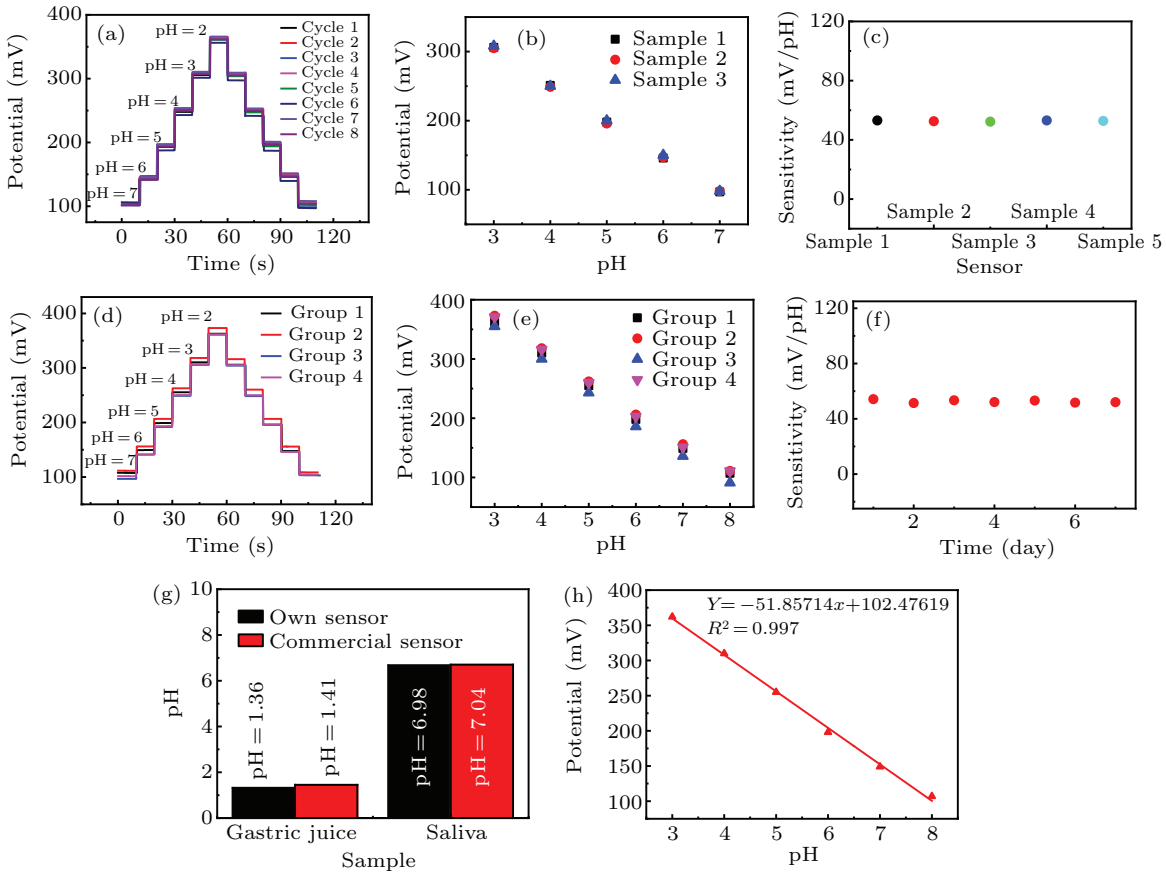


Fig. 5. General performance and response of pH sensors prepared in the same batch: (a) test pH = 2–7 step repeatability; (b) linear response of materials from different groups; (c) sensitivity to pH response. General performance and response of pH sensors prepared in different batches: (d) test pH = 2–7 step repeatability; (e) linear response of materials from different groups; (f) durability/stability study of the sensor; (g) comparison of the prepared pH sensor and the commercial pH sensor, the linear curve of the prepared pH sensor; (h) fitting equation.

Next, the practicability of the PdNPs/NC-500-modified sensor was investigated using two biological samples, namely, gastric juice and saliva. To perform a real sample analysis, we purchased artificial saliva and gastric juice samples from a hospital. Here, the comparative judgment between the results obtained by the sensor and the results obtained by commercial pH sensors were correlated. Figures 5(g) and 5(h) show the responses obtained by the PdNPs/NC-500-modified pH sensor and commercial pH sensor. The pH values of saliva and gastric juice measured using the prepared pH sensor showed that the maximum changes in gastric juice and saliva compared with the commercial pH meter (0.72% and 2.09%, respectively), which are relatively smaller than the normal pH range of body fluids. The calculated standard calibration curve showed a linear response of $R^2 = 0.997$, which indicates the accuracy of the prepared pH sensors. The major hurdle in the quantitative detection of body fluids using this two-electrode pH sensor is the accumulation of Cl^- on the surface of the Ag/AgCl reference electrode. This problem has been overcome using the PVB-based Ag/AgCl reference electrode, in which PVB coating with high Cl^- content was prepared, which provided stable Cl^-. In principle, this modification in the reference electrode allows the Cl^- concentration to reach dynamic equilibrium and diminishes the effect arisen due to the concentration change of Cl^-. A flexible reference electrode was prepared with high polymer-coated KCl powder. Its stability, sensitivity, and anti-interference performance were as good as that of the saturated calomel electrode.

4. Summary

The study showed the *in-situ* preparation of the PdNPs/NC composite material using WK as a precursor. The *in-situ* prepared PdNPs played a key role in the controlled switching of protein structure to the N-doped carbon skeleton with π–π arrangement at the mesoscale level that mimics A–B polymeric structure; hence, highly susceptible to H^+ ions.[3] The choice of WK is based on its singular molecular structure having tertiary amino acid sequence and disulfide cross-linkage, which not only helps in the preparation of PdNPs but also acts as a precursor for activated N-doped aromatized carbon preparation.[10] The *in-situ* synthesized PdNPs play an essential role in the carbonization process, in which PdNPs showed a catalytic effect in pyrolysis and CO_2 emission to acquire aromatized carbon structure.[11] WK was the best precursor for the synthesis of the N-doped carbon skeleton with the π–π arrangement, which mimics the A–B type polymeric structure; hence, highly susceptible to H^+ ions. A series of materials were prepared by temperature variation and used for the fabrication of different strip-based solid-state pH sensors. The PdNPs/NC-500-modified sensor exhibited the highest pH sensitivity with excellent stability and durability. The optimized pH sensor showed high specificity, selectivity, and durability with the sensitivity of 55 mV/pH unit and the RSD of 0.79%. The sensor was useful for biological samples, namely, saliva and gastric juices.

Acknowledgements

Project supported by the National Natural Science Foundation of China (Grant Nos. 51502253, U1405226, 21503175, and 21705135), Natural Science Foundation of Guangdong Province, China (Grant No. 2016A030310369), and Natural Science Foundation of Fujian Province, China (Grant No. 2017J01104). The authors also thank the technical supports from Chhaya Panase (Principal M. D. College).

References

[1] Broza Y Y, Zhou X, Yuan M, Qu D, Zheng Y, Vishinkin R, Khatib M, Wu W and Haick H 2019 *Chem. Rev.* **119** 11761
[2] Bandodkar A J, Hung V W S, Jia W, Valdés-Ramírez G, Windmiller J R, Martinez A G and Ramírez J 2013 *Analyst* **138** 123
[3] Patil, A B, Meng Z H, Wu R H, Ma L Y, Xu Z J, Shi C Y, Qiu W, Liu Q and Zhang Y F 2020 *Nanomicro Lett.* **12** 117
[4] Curto V F, Fay C, Coyle S, Byrne R, O'Toole C, Barry C, Hughes S, Moyna N and Diamond D 2012 *Sensor. Actuator. B: Chem.* **171** 1327
[5] Guinovart T, Valdés-Ramírez G, Windmiller J R, Andrade F J and Wang J 2014 *Electroanalysis* **26** 1345
[6] Urban G, Jobst G, Keplinger F, Aschauer E, Tilado O, Fasching R and Kohl F 1992 *Biosens. Bioelectron.* **7** 733
[7] Nyein H Y Y, Gao W, Shahpar Z, Emaminejad S, Challa S, Chen K and Fahad H M 2016 *ACS Nano* **10** 7216
[8] Oh S Y, Hong S Y, Jeong Y R, Yun J, Park H, Jin S W, Lee G, Oh J H and Lee H 2018 *ACS Appl. Mater. Interfaces* **10** 13729
[9] Manjakkal L, Szwagierczak D and Dahiya R 2020 *Prog. Mater. Sci.* **109** 100635
[10] Ma L Y, Patil A B, Wu R H, Zhang Y F, Meng Z H, Zhang W L, Kong L Q, Liu X Y and Wang J 2021 *Nanotechnology* **22** 739
[11] Patil A B, Zheng C, Ma L Y, Wu R H, Mengane S K, Zhang Y F, Liu X, Meng Z H, Zhang W L, Xu Z J, Chen C, Huang J N and Liu X Y 2020 *Nanotechnology* **32** 065502
[12] Shi C Y, Xing Y, Patil A, Meng Z H, Yu R, Lin N B, Qiu W, Hu F and Liu X Y 2019 *ACS Appl. Mater. Interfaces* **11** 30125
[13] Wang Q, Jian M, Wang C and Zhang Y 2017 *Adv. Funct. Mater.* **27** 1605657
[14] Zhu S, Zeng W, Meng Z, Luo W, Ma L Y, Li Y and Lin C 2019 *Adv. Mater.* **31** 1900870
[15] Patil A B, Huang Y F, Ma L Y, Wu R H, Meng Z H, Kong L Q, Zhang Y F, Zhang W L, Liu Q and Liu X Y 2019 *Biosens. Bioelectron.* **142** 111595
[16] Angin D 2014 *Fuel* **115** 804
[17] Salvo P, Calisi N, Melai B, Cortigiani B, Mannini M, Caneschi A, Lorenzetti G, Paoletti C and Lomonaco T 2017 *Biosens. Bioelectron.* **91** 870
[18] Kim D M, Cho S J, Cho C H, Kim K B, Kim M Y and Shim Y B 2016 *Biosens. Bioelectron.* **79** 165
[19] Hekmati M, Bonyasi F and Javaheri H 2017 *Appl. Organomet. Chem.* **31** 132
[20] Zhuiykov S 2012 *Sensor. Actuator. B: Chem.* **161** 1